Kinetic instabilities in substorm dynamics

W. Horton, J.-H. Kim, E. Spencer, and C. Crabtree

Abstract: A brief survey is given of the kinetic theory of plasma instabilities that are potentially important in substorm dynamics. Instabilities associated with the release of the pressure gradients in the dipole-to-near geotail transition region are key candidates to explain the initial release of stored energy with the simultaneous onset of auroral brightening. Instabilities driven by the plasma sheet current gradient in the region beyond 15-20 $\mathrm{R_E}$ are responsible for release of lobe magnetic energy and the initiation of high speed Earthward flowing streams. Generally, either instability could occur first or both essentially simultaneous according to local plasma gradients and the $\boldsymbol{B}$-field.

Key words: Kinetic instability, Substorms, magnetic reconnection.

1. Introduction

Space science has been remarkably successful in identifying the large number of plasma instabilities that occur in the magnetosphere and ionosphere. The one central problem where the identification of the key instabilities is still controversial is the substorm dynamics. Recent advances in multiple spacecraft missions and the IMAGE space craft have defined the issues in substorm dynamics much more sharply. At the same time the kinetic theory of the key substorm instabilities has advanced dramatically. Here we review the advances made in the kinetic theory of instabilities thought to dominate the substorm problem.

There are four classes of kinetic instabilities invoked to explain the substorm growth and expansion phases. They are (1) the pressure gradient driven ballooning interchange modes with shear Alfvén wave polarization of $\delta B_\perp$ and a smaller $\delta B_\parallel$, (2) the drift compressional ballooning mode driven by the ion temperature gradient with a dominantly $\delta B_\parallel$ polarization and small $\delta B_\perp$ and electrostatic field part, (3) the large set of collisionless tearing modes driven by the gradient of the plasma current density $\partial j/\partial\psi = j'/B$ in contrast to the density and temperature gradients, (4) the cross field current driven instabilities (CCI) that require no spatial gradients but have large $v_d = j_\perp/en \geq v_i$ where $v_i = (T_i/m_i)^{1/2}$. There is a large class of current driven instabilities that are well known in the plasma literature. There is a recent review article of [18] covering the CCI instabilities. Needless to say, they can be a key player in substorm dynamics and often can appear as the nonlinear development to small space scales of the first three types of instabilities.

Technically, the tearing mode instabilities are the most difficult plasma instabilities to calculate and have been actively debated for decades. The tearing mode is ubiquitous in the laboratory tokamak plasma. While the toroidal geometry plays some role in the mode tearing many features are in common with the geomagnetic tail. The large plasma current $\mu_0 j(\psi) \to j(\psi)$ (hereafter) is confined to the core with a peaking $dj/d\psi$ that increases with time or with core heating of the electrons. Here ψ is the flux function from the magnetic field produced by the plasma current, and the external coil driven toroidal field B_T drops out of the tearing mode stability problem except for determining the location of the $k_\parallel = 0$ surfaces. The situation is the same with the B_y field component in the geomagnetic tail. The standard tearing mode theory is given in [3] and involves the solution of the zero frequency shear Alfvén mode equation around the field reversing current layer of width L_z. Here we use the GSM coordinates of the geomagnetic tail. The solution of the field structure gives the logarithmic derivative of the perturbed flux function $\delta\psi$ with $\Delta' = (d\delta\psi/dz)/\delta\psi$ at the tearing layer. The value of Δ' is negative for stable modes, crosses zero for unstable modes and goes to infinity as the plasma becomes ideal MHD unstable from the pressure gradient exceeding the critical $dp/d\psi$ of the ballooning modes. These features are seen in the magnetic field and core soft x-ray spectrometers of tokamaks as in [4]. The lowest magnetic mode m/n=1/1 shows the sawteeth crashes at intervals of about 100 Alfvén periods and the 3/2 mode is stable but repeatedly kicked or seeded by the pulses from the 1/1 mode. Finally, as the core plasma pressure rises high enough the 3/2 mode catches on and grows to form a large magnetic island.

Qualitatively, the description of this evolution of the stability of the tearing mode is seen from the formula for $\Delta' = -2k_z \cot(k_z L_z)$ where $k_z = (dj/d\psi - k_x^2)^{1/2}$. As the current density gradient increases so that $k_z L_z \to \pi$ the Δ' goes to infinity and the island width is observed to grow to the size that is comparable to the scale L_z of the current layer width. In kinetic theory of collisionless tearing modes it is not necessary to introduce the Δ' of the external solutions when the whole region of the tearing mode function is treated globally. As we will see, the lack of a full global treatment of the tearing mode led to a long term misconception about the mode being more stable than it is known from recent kinetic theory calculations and simulations.

In this article, we first describe the state of the kinetic ballooning mode instability and the drift compressional mode instability in Sec. 2. In Sec. 3 we describe the current understanding of the collisionless tearing modes which is a complex field. There are basically two scales of the tearing mode instability, that of the ion tearing mode and that of the electron mode. Both modes have been seen in high resolution simulations which are again too wide a topic to summarize here. The ion tearing mode is considerably more unstable than was presented by [16] as is acknowledged in [24]. The electron tearing mode is

Received 5 June 2005.

W. Horton, J.-H. Kim, and E. Spencer. Institute for Fusion Studies, The University of Texas at Austin
C. Crabtree. Laboratory for Nuclear Science, MIT

easier to simulate and discuss since the ions play only the role of quasineutrality here. We give an electron tearing mode simulation with the electron Hall terms of the skin depth and the ion inertial scale length that shows a 60% conversion of stored magnetic energy into electron particle energies in a period of 50 Alfvén times which is sufficiently fast and strong to be a dominant energy release mechanism in the growth phase of a substorm.

2. Kinetic Ballooning Interchange Instabilities

The kinetic theory of the drift ballooning interchange modes require bounce averaged response to both the electron and ion perturbed distribution function $\delta f_e(\epsilon, \mu, \boldsymbol{x}, t)$ and $\delta f_i(\epsilon, \mu, \boldsymbol{x}, t)$ where μ is the magnetic moment $\mu = v_\perp^2/2B$ and ϵ the kinetic energy per unit mass $\epsilon = v^2/2$.

The ballooning interchange maximum growth rate is approximately $\gamma_{max} = 0.1 v_i/(L_p R_c)^{1/2}$ where L_p is the ion pressure gradient scale length defined by $1/L_p = \partial \ln p_i/\partial x$ and R_c is the minimum radius of curvature which is given by $\kappa(x, z = 0) = B_x'/B_n = 1/R_c$. This growth computed as a function of distance down the geomagnetic tail reaches a maximum in the region $x = -6$ to $-10\,\mathrm{R_E}$ where the Earthward pressure gradient is steepest.

In the plasma sheet the local magnetic field is given by $\boldsymbol{B} = B_x(z)\hat{\mathbf{x}} + B_n\hat{\mathbf{z}}$ where $|z| \le L_z$. At the edge of the central plasma sheet $|z| = L_z$ the field is $\boldsymbol{B} = B_{x0}\hat{\mathbf{x}} + B_n\hat{\mathbf{z}}$. In the CPS the local B-field magnitude varies as $B = (B_n^2 + B_x'^2 z^2)^{1/2}$ with a large mirror ratio $R_m = B_{x0}/B_n \ge 10$ where $B_{x0} = B_x(z = L_z) = B_x' L_z$ is the lobe magnetic field. Pressure balance across the central plasma sheet gives $B_{x0}^2/2\mu_0 = p_0 \approx n_0 T_i$. Thus there is a very high ratio of local plasma pressure-to-magnetic field energy density at the equatorial plane $\beta = 2\mu_0 p_0/B_n^2 = (B_{x0}^2/B_n^2) \ge 100$. Owing to the high mirror ratio R_m, ions and electrons with pitch-angles greater than $\alpha \approx 15^\circ$ mirror in the CPS and the ballooning eigenfunctions are confined to the CPS.

[8] solved the integral equation for the ballooning drift-Alfvén eigenmodes and show that these modes first go unstable in the transitional region $X = -6$ to $-10\,\mathrm{R_E}$ where the $\boldsymbol{\nabla} p_i/pR_c$ is maximized and $\beta < 10$. Closer to the Earth the large value of $k_\parallel^2 v_A^2$ from the short connection length $\pi/k_\parallel$ stabilizes the interchange modes. Deep into the geomagnetic tail for $X \le -10\mathrm{R_E}$ the plasma compressional energy in the interchange motion overcomes the destabilization from the interchange energy released. Similar results are given in [6].

Kinetic theory predicts that as the Earthward pressure gradient increases the first mode to go unstable is the ballooning interchange mode in the region that maps to the auroral brightening zone. This pressure-gradient instability releases a pressure pulse $\delta p > 0$ with $\delta B_z < 0$ that propagates tailward and typically sets off magnetic reconnection in the tail at $X = -20$ to $-25\,\mathrm{R_E}$. This regime is called the inside-out model of substorm.

[7] considered the finite-gyroradius effects on drift compressional modes. Drift-Compressional modes (DCM) are similar to Drift-Mirror modes (DM) in that they are dominated by the compressional part $\delta B_\parallel$ of the polarization. However DCM have as their source of free energy spatial inhomogeneities whereas DM rely on temperature anisotropy to drive the mode unstable. Crabtree and Chen used the ratio of the electron temperature to the ion temperature as a small parameter to decouple the electrostatic component from the compressional component. They also considered frequencies below the shear Alfvén frequency which eliminates the coupling between the compressional component and the shear component of the perturbed magnetic field. With these orderings the following integral eigenvalue problem was derived

$$k_\perp^2 \rho_i^2 \delta B_\parallel + \beta_i \left\langle \epsilon\lambda \left[\frac{\omega - \omega_{*ti}}{\omega - \overline{\omega}_{Di}}\right] \overline{\left(\delta B_\parallel \sqrt{\overline{B}} J_1\right)} \sqrt{\overline{B}} J_1 \right\rangle = 0. \tag{1}$$

where the angle brackets refer to velocity space integrations and the overline refers to bounce-averaging along the field line $\overline{F} = 1/\tau \int_{-s_t}^{s_t} F ds/v_\parallel(\epsilon, \mu, s)$, s_t is the turning point in the mirror field. Also ω_{*ti} is the ion diamagnetic drift frequency containing the ion pressure gradient, $\overline{\omega}_{Di}$ is the grad-B/curvature drift frequency averaged over the bounce motion and η_i is $\eta_i = \partial \ln T_i/\partial \ln n_i$ is the ion temperature gradient relative to the ion density gradient, and J_1 is the finite-gyroradius Bessel

This equation was solved numerically and analytically. Maximal growth rates were found to occur when $k_\perp \rho_i \sim \mathrm{O}(1)$, with $\gamma_{max} \sim v_i(\eta_i - 2/3)/R_c$ and for $\eta_i \sim -1$. The radial mode width may also be estimated as $\sqrt{\rho_i}$. [11] studied the kinetic generalization of the standard MHD ballooning equation studied by [15] and others. From a quadratic form in the drift-kinetic approximation a reduced kinetically correct quadratic form was derived that accounted for the strong coupling between the shear Alfvén wave with the interchange dynamics given by,

$$\begin{aligned}
&\int d\psi dy \int \frac{ds}{B}\Big[-\frac{\omega^2}{v_A^2}\left|\xi^\psi\right|^2 + \frac{1}{\mu_0}\left|\frac{\partial \xi^\psi}{\partial s}\right|^2 + \frac{1}{\mu_0}\left|Q_L^{(0)}\right|^2 \\
&-\frac{2\mu_0 p' \boldsymbol{\kappa}\cdot\nabla\psi}{B^2}\left|\xi^\psi\right|^2 \\
&-4\pi\sum_a \int d^3v \,\frac{\partial F_a}{\partial \epsilon}\left(\frac{\omega - \omega_{*a}}{\omega}\right)\left|\mu\overline{Q_L^{(1)}}\right|^2 \\
&+i\pi(4\pi)\sum_a \int d^3v \,\frac{\partial F_a}{\partial \epsilon}(\omega - \omega_{*a})\delta(\omega - \omega_{Da})\left|\mu\overline{Q_L^{(1)}}\right|^2\Big] \\
&= 0.
\end{aligned} \tag{2}$$

Here ξ^ψ is the contravariant component of the displacement ($\xi^\psi = -ik_y\chi$) of the perturbed flux tube that is the kinetic theory generalization of the MHD displacement field $X(s)$. Here $Q_L^{(0)}$ and $Q_L^{(1)}$ are functions of ξ^ψ so that Eq. (2) contains only one field variable, as in MHD theory. This kinetic theory is given in [30].

3. Magnetic Reconnection Instabilities

The reversed magnetic field $\pm B_{x0}$ in the geotail is a large reservoir of energy available energy to drive plasma flows and to increase the thermal energies. These tearing modes are of two types :

- microscale electron tearing modes on the scale of $c/\omega_{pe} \sim 10\,\mathrm{km}$ and
- the marcoscale tearing modes on the scale of $c/\omega_{pi} \sim \rho_i \sim 400\,\mathrm{km}$.

There must be and can be hundreds of the c/ω_{pe}-scale tearing mode sites to release the required magnetic energy to explain substorms. The ion tearing mode sites will be of the order of a few. The electron modes grow very fast on the time scale of seconds whereas the ion tearing modes require minutes.

3.1. Ion Scale Tearing Modes

Tearing models occurring on the ion gyroradius scale are difficult to analyze theoretically due to fast bounce motion of electrons with period $\tau = \int_{-s_t}^{s_t} ds/v_\parallel(\epsilon,\mu,s)$ that yields an integral response for the perturbed plasma density δn and current δj in the ion tearing dynamics. The ion tearing mode growth rate γ_k^i is given by

$$\gamma_k^i = k_x v_i \left(\frac{c^2}{\omega_{pi}^2}\right)\frac{\Delta_k'}{L_z} = \omega_{cxo}\left(\frac{\rho_i}{L_z}\right)^3 , \tag{3}$$

where $\omega_{cxo} = eB_x/m_i = 2\,\mathrm{rad/s}$ for $B_x = 20\mathrm{nT}$ lobe field. When the current sheet thickness exceeds $L_z = 3\rho_i$, the growth rate is too slow to play a role in the substorm dynamics.

Using the quasineutrality condition [28]

$$\frac{e\phi_1}{T_i}n_0 + \tilde{n}_1 = 0 \tag{4}$$

and integrating over velocity space the trapped and transient contribution to the total perturbed electron distribution yields the perturbed electron density

$$\tilde{n}_1 = (\ll n_e \gg - n_e)\frac{e\phi_1}{T_e} + \frac{\delta n_e}{\delta A}A_1 \tag{5}$$

where the vector potential contribution term $(\delta n_e/\delta A)\delta A_1$ is given in detail in [29].

The key point is to include the contribution of the perturbed density over the long flux tube where the small pitch angle electrons make long excursions toward the ionosphere. Previous simulations in [5] and [25] may not have included sufficiently long flux tubes to capture this physics.

3.2. Electron Scale Tearing Modes

The latest developments on the electron-scale magnetic reconnection (MR) modes are given in [1] and [23]. The impulsive reconnection model of Bhattacharjee has the field-line-breaking mechanism of electron inertial given by finite $d_e = c/\omega_{pe}$. Therefore, it is necessary to use the generalized Ohm's Law

$$\boldsymbol{E} + \boldsymbol{v}\times\boldsymbol{B} = \frac{c^2\mu_0}{\omega_{pe}^2}\frac{d\boldsymbol{J}}{dt} - \frac{\boldsymbol{\nabla} p_e}{ne} + \frac{\boldsymbol{J}\times\boldsymbol{B}}{ne} + \eta\boldsymbol{J} \tag{6}$$

where $\boldsymbol{E}$ is the electric field, $\boldsymbol{B}$ is the magnetic field, $\boldsymbol{v}$ is the plasma flow velocity, c is the speed of light, $\boldsymbol{J}$ is the current density, p_e is the electron pressure, ω_{pe} is the electron plasma frequency, n is the electron density, e is the magnitude of the electron charge.

In the simulations shown here we take the limit of zero plasma resistivity η and check energy conservation to five digits. With high order time integrators it is possible to run for finite times with zero resistivity. The dynamics exhibits a long exponential growth time ending with a nonlinear, faster than linear exponential growth pulse that saturates into a coherent nonlinear structure. Typically 50-60% of the initial magnetic energy is redistributed into the sum of the parallel and perpendicular flow energies and the electron thermal pressure by the reconnection pulse.

The simplest electron tearing mode dynamics occurs when plasma flow is almost incompressible. This occurs when there is a guide field B_y. The small flow compression comes from the polarization drift of the ions and is given by $\partial U/\partial t$ where $U = \nabla_\perp^2\phi$ with $\boldsymbol{E} = -\boldsymbol{\nabla}\phi$ and $\boldsymbol{B} = \hat{\mathbf{y}}\times\boldsymbol{\nabla}\psi + B_y\hat{\mathbf{y}}$. The vorticity U grows to feed plasma into the reconnection layer. The compressional Alfvén wave propagates drops out of the dynamics in this regime owing to its higher frequency and different polarization. The plasma is described in an electron-Hall fluid limit by the following two field equations

$$\frac{\partial F}{\partial t} + [\phi, F] = \rho_s^2[U,\psi] \tag{7}$$

$$\frac{\partial U}{\partial t} + [\phi, U] = [J,\psi] \tag{8}$$

where $J = -\nabla_\perp^2\psi$, $F = \psi + d_e^2 J$, $U = \nabla_\perp^2\phi$, and the Poisson bracket is defined by $[\phi, F] = \hat{\mathbf{y}}\cdot\boldsymbol{\nabla}\phi\times\boldsymbol{\nabla}F$. All quantities are dimensionless(this will be fixed with the proper dimensions). The distance is normalized by the system size L_z and time is normalized by Alfvén time scale $\tau_A = L_z/v_A$ where the Alfvén velocity $v_A = \sqrt{B^2/2\mu_0\rho}$. Also two dimensionless parameters d_e and ρ_s are the electron skin depth $d_e = (c/\omega_{pe})/L_z$ and the ion sound gyro radius $\rho_s = (c_s/\omega_{ci})/L_z$.

The computation has been done with

$$\psi = \Sigma_{n,m}\psi_{m,n}(t)\exp(inz + im\epsilon x) \tag{9}$$

$$\phi = \Sigma_{n,m}\phi_{m,n}(t)\exp(inz + im\epsilon x) \tag{10}$$

where $n,\ m$ are integers, $\epsilon = L_z/L_x$ is an aspect ratio of the system. The initial profile are the unstable current sheet $\psi_{1,0}$ with small perturbations $\psi_{4,1}$ and $\phi_{4,1}$, that is,

$$\psi(0) = \cos z + \delta\psi\cos(4z)\cos(\epsilon x)$$
$$\phi(0) = \delta\phi\sin(4z)\sin(\epsilon x)\,.$$

The electron model conserves the total energy of electrons and the magnetic field. The energy formula and the conservation law are given by

$$\begin{aligned}\frac{dE_{tot}}{dt} &= \frac{d}{dt}\left(E_B + E_\parallel + E_{E\times B} + E_p\right)\\ &= \frac{1}{2}\frac{d}{dt}\int dxdz[(\boldsymbol{\nabla}\psi)^2 + d_e^2(\nabla^2\psi)^2\\ &\qquad +(\boldsymbol{\nabla}\phi)^2 + \rho_s^2(\nabla^2\phi)^2] = 0\end{aligned} \tag{11}$$

where E_B is magnetic energy, $E_\parallel$ is electron parallel flow energy, $E_{E\times B}$ is the electron perpendicular flow energy and E_p

is the electron thermal energy. As shown in Fig. (1), there are four transfers between the different energy components. The magnetic energy E_B and the electron parallel flow energy $E_{\|}$ are transfered back and forth to the thermal energy E_p by thermal interaction $< v_{e\|}\nabla_{\|}p_e >$. And the energies, E_B and $E_{\|}$, are transfered back and forth to the perpendicular flow energy $E_{E\times B}$ by the electric interaction $< j_{\|}\nabla_{\|}\phi >$.

The energy change relevant to the ϕ, U, ψ and J are shown in Fig. (2), During the process, almost 60% of the magnetic energy is released and About 30% of the released energy is transfered to the ion thermal energy. The simulation box is $20\pi\, c/\omega_{pe} \times 40\pi\, c/\omega_{pe}$ and the unit of energy is $E_0 = B_0^2 L_z^2/2\mu_o$ which for 10 nT reversed field over a $L_z = 10\, c/\omega_{pe} = 100\mathrm{km}$ is $2.5 \times 10^6\, \mathrm{J/R_E}$. In the upper panel, we see the released magnetic energy ΔE_B of $12\, E_0$ and the increase of the parallel flow kinetic energy in the electrons is $5\, E_0$. In the bottom panel the perpendicular flow energy increases first to $8, E_0$ and then drops to $2\, E_0$ while the electron thermal energy continually increases to $5\, E_0$. Energy is conserved by the 12 units of released magnetic energy going to 5+2+5 units of parallel flow, perpendicular flow and thermal plasma energies. In terms of fractional changes this is approximately a 60% decrease of magnetic energy transformed into 10% $E\times B$ flow, 25% parallel flow and 25% electron thermal energy. The space and time scales are $10\, c/\omega_{pe}$ and $60 L_z/v_A$. In the central plasma sheet these scales are typically 100 km and 1 min.

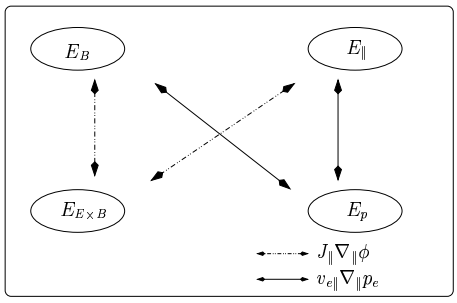

Fig. 1. Diagram of the energy transfer among magnetic energy E_B, perpendicular kinetic energy $E_{E\times B}$, parallel kinetic energy $E_{\|}$ and electron thermal energy E_p.

3.3. Global Driven Reconnection Model

The solutions described above are for local instability of the current sheet with the growth rate driven by the gradient of the current density $dj_y/d\psi$. The wave functions are localized at the current sheet dropping off to negligible values in the lobe plasma. There is another type of global driven reconnection solution that is obtained by changing the exterior boundary conditions. In the global solution the boundary conditions are changed to be those given on the upper and lower magnetopause with mixed values of $\delta\psi$ and $d\delta\psi/dz$ at $z = \pm H$. These are called driven reconnection solutions and are used in [9] and [10]. These global solutions are those that are created in the driven reconnection simulations of [26] and [2].

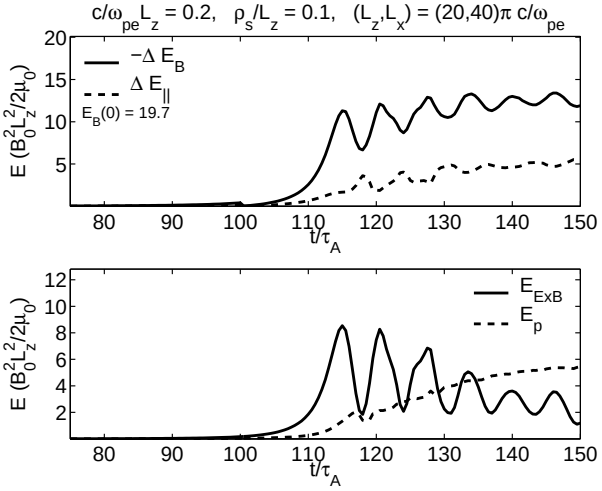

Fig. 2. Plot of energy evolution in time for $d_e = 0.2, \rho_s = 0.1$ with initial mode $(k_z, k_x) = 2\pi(4, 0.5)/L_z$. Almost 60% of magnetic energy is released.

4. Crossfield Current Drive Instabilities

In the driven reconnection simulations, and other plasma sheet instabilities including the firehose instability driven by the bursty bulk flows ([13, 14] and [12]), the gradient of the magnetic field is locally very large and the associated drift velocity $v_d = j/en_e \geq v_i = \sqrt{T_i/m_i}$ locally. This condition when satisfied over a region of sufficient volume gives rise to the crossfield current driven instabilities called CCI. Lui and his collaborators [19, 20, 21] have worked out many details of the CCI instabilities and have shown them to be capable of producing a turbulent resistivity that increases the local electric field in proportional to the level of these fluctuations. [17] gives a review of these instabilities and their effects on the currents in the plasma connected to the regions of auroral brightenings. The Geotail space data in this region of 10-13 R_E shows strong magnetic field fluctuations as shown for five substorms in detail in [27].

5. Conclusion

Thus we see there are three classes of kinetic instabilities that can be associated with substorm expansion phases. The most widely used instabilities are the pressure gradient driven ballooning interchange mode in the near Earth transitional region between the dipole field and the inner edge of the central plasma sheet. Transient conditions of either sharply increasing or decreasing convection electric field from the interplanetary magnetic and electric field create the steep Earthward pressure gradient to trigger this strong instability with growth periods of the order of minutes. The growth rate divided by the local proton cyclotron frequency is of order the proton gyroradius divided by the geometric mean of the plasma pressure scale length L_p and the local radius of magnetic curvature.

In the midtail region, which is stable to the ballooning interchange mode owing to the high local plasma pressure, the first instability to be excited is the ion scale tearing mode. The ion tearing mode occurs when the current gradient scale length L_z

is sufficiently short estimated here as three ion gyroradii in the lobe field B_{x0} and $B_n/B_{x0} \leq 0.1$. The mode produces a large magnetic island but grows slowly with the growth rate divided by the lobe cyclotron frequency proportional to the third power of ρ_i/L_z, that is $\gamma_{max}/\omega_{ci} \sim (\rho_i/L_z)^3$.

When local current filaments of size less than the proton gyroradius are present then the electron scale tearing mode is driven unstable. The electron tearing mode grows very rapidly with time scales of seconds but the magnetic islands are small scaling with the electron collisionless skin depth d_e which is tens of kilometers.

We show a simulation for these small scale tearing modes that gives a conversion of 60% of the magnetic energy into electron thermal energy and electron parallel and perpendicular flow energies. There would be a high mode density $d^3\boldsymbol{k}$ of the electron tearing modes, and they are not restricted to the symmetry plane of the geomagnetic tail but can occur locally wherever the local gradient of the current density dj_y/dz is sufficiently strong. On the dayside magnetopause [22] shows evidence for a high density of electron reconnection sites.

Finally, the current density itself, without a gradient, can produce a high frequency kinetic instabilities that produce turbulent scattering of the electrons that create an anomalous resistivity. There is a wide variety of these instabilities that go under the name of CCI (crossfield current instabilities) as reviewed by [18]. It seems likely that all three types of instabilities are active in various types and stages of the substorm dynamics.

With the THEMIS mission and then the MMS mission we may expect to learn which type of instability is dominant in various types of substorms and responsible for which effects such as conversion of magnetic energy to various forms of ion and electron energies.

Acknowledgements

This work is supported by the NSF Grant ATM-0539099.

References

1. Bhattacharjee, A., K. Germaschewski, and C. S. Ng, Current singularities : Drivers of impulsive reconnection, *Phys. Plasmas*, *12*, 042,305, 2005.
2. Biskamp, D., Magnetic reconnection via current sheets, *Phys. Fluids*, *25*(5), 1520–1531, 1986.
3. Biskamp, D., *Magnetic Reconnection in Plasmas*, chap. 4, pp. 82 – 95, Cambridge Univerity Press, 2000.
4. Brennan, D. P., et al., A mechanism for tearing onset near ideal stability boundaries, *Phys. Plasmas*, *10*(5), 1643–1652, 2003.
5. Brittnacher, M., K. B. Quest, and H. Karimabadi, A new approach to the linear theory of single-species tearing in two-dimensional quasi-neutral sheets, *J. Geophys. Res.*, *100*(A3), 3551–3562, 1995.
6. Cheng, C. Z., and A. Lui, Kinetic ballooning instability for substorm onset and current disruption observed by ampte/cce, *Geophys. Res. Lett.*, *25*(21), 4091, 1998.
7. Crabtree, C., and L. Chen, Finite gyroradius theory of drift compressional modes, *Geophys. Res. Lett.*, *31*(L1), 7804, 2004.
8. Crabtree, C., W. Horton, H. V. Wong, and J. W. V. Dam, Bounce-averaged stability of compressional modes in geotail flux tubes, *J. Geophys. Res.*, *108*, 1084, 2003.
9. Hahm, T., and R. Kulsrud, Forced magnetic reconnection, *Phys. Fluids*, *28*(8), 2412–2418, 1985.
10. Horton, W., and T. Tajima, Linear theory of driven reconnection, *J. Geophys. Res.*, *93*(A4), 2741–2748, 1988.
11. Horton, W., H. V. Wong, J. W. V. Dam, and C. Crabtree, Stability properties of high-pressure geotail flux tubes, *J. Geophys. Res.*, *106*(A9), 18,803–18,822, 2001.
12. Horton, W., B.-Y. Xu, H. Wong, and J. V. Dam, Nonlinear dynamics of the firehose instability in a magnetic dipole geotail, *J. Geophys. Res.*, *109*(A0), 9216, 2004.
13. Ji, S., and R. Wolf, Double-adiabatic-MHD theory for motion of a thin magnetic filament and possible implications for bursty bulk flows, *J. Geophys. Res.*, *108*(A5), 1191, 2003.
14. Ji, S., and R. Wolf, Firehose instability near substorm expansion phase onset?, *Geophys. Res. Lett.*, *30*(24), 2242, 2003.
15. Lee, D.-Y., and R. A. Wolf, Is the earth's magnetotail balloon unstable, *J. Geophys. Res.*, *97*(A12), 19,251–19,257, 1992.
16. Lembege, B., and R. Pellat, Stabiity of a thick two-dimensional quasineutral sheet, *Phys. Fluids*, *25*(11), 1995–2004, 1982.
17. Lui, A., Current disruption in the earth's magnetosphere : Obserbation and models, *J. Geophys. Res.*, *101*(A6), 13,067–13,088, 1996.
18. Lui, A., Potential plasma instabilities for substorm expansion onsets, *Space Sc. Reviews*, *113*(1), 127–206, 2004.
19. Lui, A., L. Frank, K. Ackerson, C. I. Meng, and S.-I. Akasofu, Systemic study of plasma flow during plasma sheet thinnings, *J. Geophys. Res.*, *82*, 4815–4825, 1977.
20. Lui, A., C. Chang, A. Mankofsky, H. Wong, and D. Winske, A cross-field current instability for substorm expansions, *J. Geophys. Res.*, *96*(A7), 11,389–11,401, 1991.
21. Lui, A., et al., Current disruptions in the near-earth neutral sheet region, *J. Geophys. Res.*, *97*(A2), 1461–1480, 1992.
22. Mozer, F., Criteria for and statistics of electon diffusion regions associated with subsolar magnetic field reconnection, *J. Geophys. Res.*, *110*(A1), 2222, 2005.
23. Ottaviani, M., and F. Porcelli, Fast nonlinear magnetic reconnection, *Phys. Plasmas*, *2*(11), 4104–4117, 1995.
24. Pellat, R., O. A. Hurricane, and J. Luciani, New mechanism for three-dimensional current dissipation/reconnection in astrophysical plasmas, *Phys. Rev. Lett.*, *77*(21), 4353, 1996.
25. Pritchett, P., and F. Coroniti, The role of the drift kink mode in destabilizing thin current sheets, *J. Geomagn. Geoelectr.*, *48*, 833, 1996.
26. Sato, T., and T. Hayashi, Externally driven magnetic reconnection and a powerful magnetic energy converter, *Phys. Fluids*, *22*(6), 1189–1202, 1979.
27. Sigsbee, K., C. A. Cattell, D. Fairfield, K. Tsuruda, and S. Kokubun, Geotail observation of low-frequency waves and high-speed earthward flows during substorm onsets in the near magnetotail from 10 to 13 r_e, *J. Geophys. Res.*, *107*(A7), 1141, 2002.
28. Sitnov, M. I., H. V. Malova, and A. S. Sharma, Role of the temperature ratio in the linear stability of the quasi-neutral sheet tearing mode, *Geophys. Res. Lett.*, *25*(3), 269–272, 1998.
29. Sitnov, M. I., A. S. Sharma, P. N. Guzdar, and P. H. Yoon, Reconnection onset in the tail of earth's magnetosphere, *J. Geophys. Res.*, *107*(A9), 1256, 2002.

30. Wong, H. V., W. Horton, J. V. Dam, and C. Crabtree, Low frequency stability of geotail plasma, *Phys. Plasmas*, *8*(5), 2415–2424, 2001.